Auditory event-related responses are generated independently of ongoing brain activity

Ville Mäkinen,* Hannu Tiitinen, and Patrick May

Apperception and Cortical Dynamics (ACD), Department of Psychology, PO Box 9, FIN-00014 University of Helsinki, Finland
BioMag Laboratory, Engineering Centre, Helsinki University Central Hospital (HUCH), Medical Engineering Centre, PO Box 340, FIN-00029 HUS, Finland

For researchers and clinical practitioners alike, evoked and event-related responses measured with MEG and EEG provide the means for studying human brain function and dysfunction. However, the generation mechanism of event-related responses remains unclear, hindering our ability to formulate viable theories of neural information processing. Event-related responses are assumed to be generated either (1) separately of ongoing, oscillatory brain activity or (2) through stimulus-induced reorganization of ongoing activity. Here, we approached this issue through examining single-trial auditory MEG data in humans. We demonstrate that phase coherence over trials observed with commonly used signal decomposition methods (e.g., wavelets) can result from both a phase-coherent state of ongoing oscillations and from the presence of a phase-coherent event-related response which is additive to ongoing oscillations. To avoid this problem, we introduce a method based on amplitude variance to establish the relationship between ongoing oscillations and event-related responses. We found that auditory stimuli do not give rise to phase reorganization of ongoing activity. Further, increases in spectral power accompany the emergence of event-related responses, and the relationship between spectral power and the amplitude of these responses can be accounted for by a linear summation of the event-related response and ongoing oscillation with a stochastically distributed phase. Thus, on the basis of our observations, auditory event-related responses are unique descriptors of neural information processing in humans, generated by processes separate from and additive to ongoing brain activity.
© 2004 Elsevier Inc. All rights reserved.

Event-related responses (ERRs; "potentials" in EEG and "fields" in MEG) are separated from ongoing brain activity and system noise by averaging measurement epochs time-locked to stimulus presentation. Ongoing activity and brain oscillations have been linked with various cognitive processes such as attention (Tiitinen et al., 1993) and sensory integration (Varela et al., 2001). Moreover, several studies have concluded that averaged ERRs are not separate from ongoing cortical processes, but rather, are generated by phase synchronization and partial phase-resetting of ongoing activity (Başar, 1980; Jansen et al., 2003; Makeig et al., 2002; Sayers et al., 1974; see Fig. 1a–d). For example, the spectral power of unaveraged EEG data appears to be independent of auditory stimulation, suggesting that ERRs result from reorganization of ongoing activity rather than from additional activity being triggered by the stimulus (Sayers et al., 1974). Further, the power of cortical oscillations at 8–13 Hz has been shown to correlate with the amplitude of ERRs (Brandt et al., 1991; Rahn and Başar, 1993a,b), indicating that the two phenomena are interlinked. However, both the amplitude of ERRs (Näätänen and Picton, 1987) and the level of ongoing brain activity (Coenen, 1998) reflect the arousal level (e.g., vigilance) of the subject. Therefore, as changes in the ERRs and in ongoing cortical activity are likely to coincide temporally, the conclusion that ongoing activity directly affects ERRs may be premature.

Methodologically, resolving this issue poses a challenge: for example, even if ERRs were generated independently of ongoing activity, the measured MEG or EEG signal would still be the sum of the two (Fig. 1e and j), and disentangling them would be far from trivial. Firstly, the oscillatory processes that make up ongoing activity are nonstationary, that is, their phase and amplitude cannot be accurately predicted from previous values (as evident in, e.g., the spontaneous fluctuations of the alpha rhythm; Laufs et al., 2003). Secondly, in analyzing oscillatory activity, limiting the frequency band sacrifices the accuracy of temporal information (time-frequency uncertainty, see e.g., Addison, 2002; Mallat, 1998). As a direct consequence, when a signal is restricted to a narrow frequency band through filtering or wavelets, a transient response whose power is distributed over a wide frequency range will inevitably affect the phase and amplitude of the ongoing oscillatory

* Corresponding author. BioMag Laboratory, Engineering Centre, Helsinki University Central Hospital (HUCH), Medical Engineering Centre, PO Box 340, FIN-00029 HUS, Finland. Fax: +358 9 471 75781.
E-mail address: ville.makinen@biomag.hus.fi (V. Mäkinen).

Available online on ScienceDirect (www.sciencedirect.com).
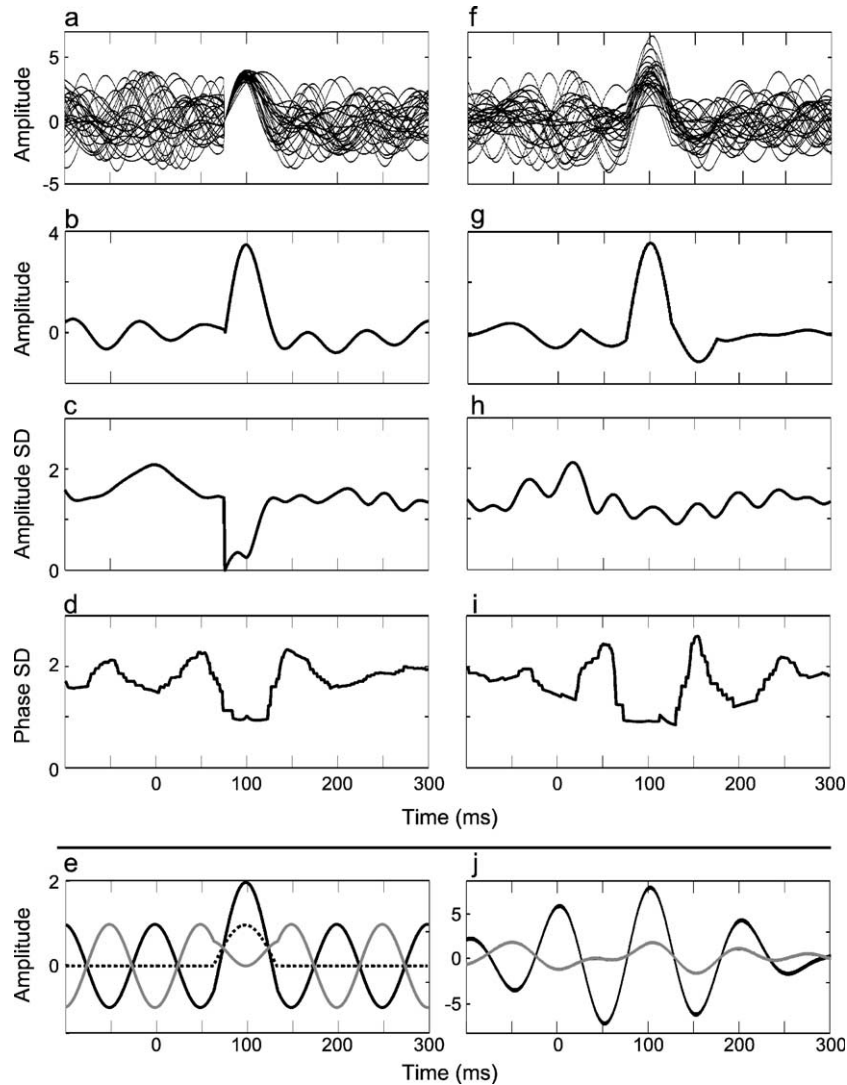
Fig. 1. Simulated data demonstrating the two possible generation mechanisms of the event-related responses (ERRs) and the stochastic summation of additive transient responses and ongoing oscillation. Reorganization of the phase distribution of ongoing oscillations as a model of ERR generation (a–d): in (a), each curve ($N = 30$) represents ongoing brain activity as a composite of four sinusoids with random initial phases and random frequencies in the 4–16 Hz range. At 75 ms, the phases of all the component sinusoids are set to zero. In (b), the averaged waveform of the curves in (a) exhibits a transient response peaking at 100 ms. In (c), the standard deviation of the amplitudes of the 30 curves in (a) is shown for each time point. This can be used as a measure of phase organization of the data: synchronization of the component sinusoids ($t = 75$ ms) is indicated by the standard deviation going to zero. The phase of the curves in (a) is obtained at each time point with a signal decomposition method (complex Morlet-wavelet, wave number = 5, center pass-band frequency 10 Hz) and the standard deviation of the phases at each time point is shown in (d). The reduced variance of the phases after 75 ms in (d) indicates the phase-coherent state of the oscillations. Transient response additive to ongoing oscillations as a model of ERR generation (e–j): In (e), a transient response (dotted curve) is triggered during ongoing, oscillatory activity. The sum of the two (representing the measured EEG or MEG signal) depends on the phase of the oscillatory activity. The black and grey curves represent the sum wave when the transient response and the oscillation are in the same and opposite phase, respectively. The two cases differ with respect to the measured peak amplitude and the power of the measured signal. In (f), the same sinusoidal signal model as in (a) is used for the curves ($N = 30$). However, no phase resetting occurs but a constant-amplitude response (a small downward deflection at 25–75 ms, followed by an upward deflection at 75–125 ms and a small downward deflection at 125–175 ms) is superposed to all trials so that in the averaged signal (g), a transient response is observed. In (h), the standard deviation of the amplitudes of the 30 curves in (f) is shown. The additive component does not change the amplitude variance of the signal. The phase of the curves in (f) is obtained with the same technique as in (d) and shown in (i). Although the ongoing oscillations are of random phase, a phase-coherent state similar to the one in (d) is observed at the latency of the transient response. This follows from the decomposition of the signal whereby the estimated phase at each time point is determined by the phase of both the ongoing oscillation and the additive component. Hence, phase estimation with signal decomposition techniques is unsuitable for studying the generation mechanisms of the ERRs. In (j), averages of five trials with highest and lowest power from (f) (black and grey curve, respectively) filtered with the Morlet-wavelet are displayed. Because filtering turns transient responses into oscillations and because stochastic summation occurs between the ongoing oscillations and the transient response, as demonstrated in (e), the oscillatory processes can be interpreted to contribute to the generation of the ERRs although, in reality, the two are independent of one another. All the panels have the same time scale; the horizontally aligned panels have the same vertical scale except in (e) and (j).

signal in its time-frequency neighborhood. Thus, by introducing temporal correlations to the signal, filtering results in artefactual predictability whereby the trial-to-trial amplitude and/or latency variance of the transient response can be determined from the phase and amplitude of the preceding ongoing oscillation although, in reality, the two may be perfectly independent. Thirdly, as demonstrated in Fig. 1, a phase-coherent state observed with signal decomposition methods (e.g., wavelets) does not imply a phase-coherent state of ongoing activity, but rather, can reflect the presence of an additive, evoked response whose phase is coherent over trials.

Explaining the generation mechanism of ERRs is essential for understanding neural information processing and the neural circuits underlying human cognition. However, explaining ERRs in terms of phase synchronization would appear problematic. Firstly, if information were contained in the synchronized state of different oscillatory processes, ongoing oscillations would stochastically (albeit rarely) produce such a state even without the presentation of a sensory stimulus. Secondly, if information processing were related to phase resetting, ongoing oscillations would stochastically be in the phase towards which they would otherwise be set and thus, the sensory stimulus would have no effect on brain activity.

Here, using MEG measurements on human subjects, we sought to establish whether ERRs are generated through phase organization of ongoing activity or through processes separate from ongoing activity. We examined the phase distribution of unaveraged MEG data using a method of amplitude-variance analysis which avoids the problems inherent in signal decomposition methods and employed a spatial filtering technique to target activity originating from auditory cortex. Spectral estimates and single-trial evaluation techniques were used to examine the influence of ongoing brain processes on the auditory ERRs.

Methods

Measurements, subjects, and basic data analysis

Nine healthy subjects were studied with their informed and written consent. The study was approved by the Ethical Committee of Helsinki University Central Hospital. The subjects watched a silent film and were under the instruction to ignore the auditory stimuli. The measurements were carried out in a magnetically shielded room with a 306-sensor MEG device (Vectorview, Elekta Neuromag Oy, Finland). The device has 204 planar gradiometer and 102 single-loop magnetometer sensors of which the gradiometers were used in the analysis because of the direct relationship between the lead-fields of the planar gradiometers and source location (Hämäläinen et al., 1993). The stimuli were binaurally delivered 750 Hz tones of 100 ms duration with 10 ms linear onset and offset ramps. The noise level inside the measurement room was 32 dB SPL (sound pressure level, A-weighted) and the stimuli were adjusted to 80 dB SPL. The stimuli were presented at least 400 times using an onset-to-onset interval of 800 ms. Both raw and online-averaged data were collected using a sampling rate of 600 Hz and a pass-band of 0.03–200 Hz. Trials with horizontal or vertical electrooculograms (EOGs) exceeding an absolute value of 150 μV were excluded from the online-averages. The data were filtered with two-way zero-phase filtering employing Chebyshev type-II infinite impulse response (IIR) filters with ≥50 dB stop-band attenuation,

optimized for maximal steepness of the roll-off using the maximum order of the filter without pass-band ripple. The right- and left-hemispheric responses were compared using the average magnitude from all the 54 sensors of the selection shown in Fig. 2 with the selection mirrored to the left hemisphere. Source visualization was performed from online-averaged data with L1 minimum-norm estimates (Uutela et al., 1999) with no region of interest (ROI) weighting.

Response source weighting (RSW) filter

The amplitude of the averaged N1m response of each sensor indicates the sensitivity of that sensor to the source of the response. This allows one to assign a value to each sensor with which the unaveraged data are weighted. This set of weights and subsequent averaging over sensors comprises a response source weighting (RSW) filter, which can be considered a derivative of signal space projection (SSP, Tesche et al., 1995) and synthetic aperture magnetometry (SAM, Vrba and Robinson, 2001). RSW filters were constructed individually for each subject and employed to the data prior to further analyses. The N1m latency for the RSW filtering process was determined from the online-averaged data of the sensor displaying maximum response amplitude. The amplitudes of the online-averaged responses from the 54 sensors were divided with the N1m peak amplitude measured at the sensor with maximum response (Fig. 2). This provided a coefficient for each sensor, and was used to weight the unaveraged data from the sensors. The weighted unaveraged data were summed over the 54 sensors. The signal-to-noise ratio (S/N) was determined as the peak amplitude of the N1m divided by the mean value of the baseline signal magnitude. The N1m and noise values were taken from absolute values of unaveraged data of all subjects and the 1–45 Hz frequency band was used for obtaining the N1m values. In subsequent analyses, the N1m peak latency was determined from the RSW-filtered data using stimulus onset time-locked averaging over all trials.

Spectral estimates, time-frequency analysis, and variance calculation

To ensure that EOG artefacts do not have different distributions in the pre- and poststimulus time windows, the unaveraged data were first divided into 800-ms data windows (starting 400 ms before stimulus onset), and those windows coinciding with >100 μV EOG amplitudes were excluded. The accepted 800-ms samples were then divided into 400-ms pre- and poststimulus data windows, which were detrended and mean-removed. Spectral estimation was performed with a nonparametric multitaper method (Percival and Walden, 1993) with zero-padded data windows (time-band width product, NW = 1.5, length of the FFT = 1024). The data from the 1–45 Hz frequency band were used in the spectral pre- and poststimulus power estimation. The mean spectral power of each specified frequency band was used when the single-trial data sorting was performed. The amplitudes and latencies of the N1m responses in the subaverages were obtained separately for each subject from a 20-ms time window centered using the peak amplitude of the data averaged over all the trials.

For the time-frequency analysis of the simulations (Fig. 1), we used a Morlet wavelet with a center frequency of 10 Hz (see, e.g., Addison, 2002; Mäkinen et al., 2004; Torrence and Compo, 1998).
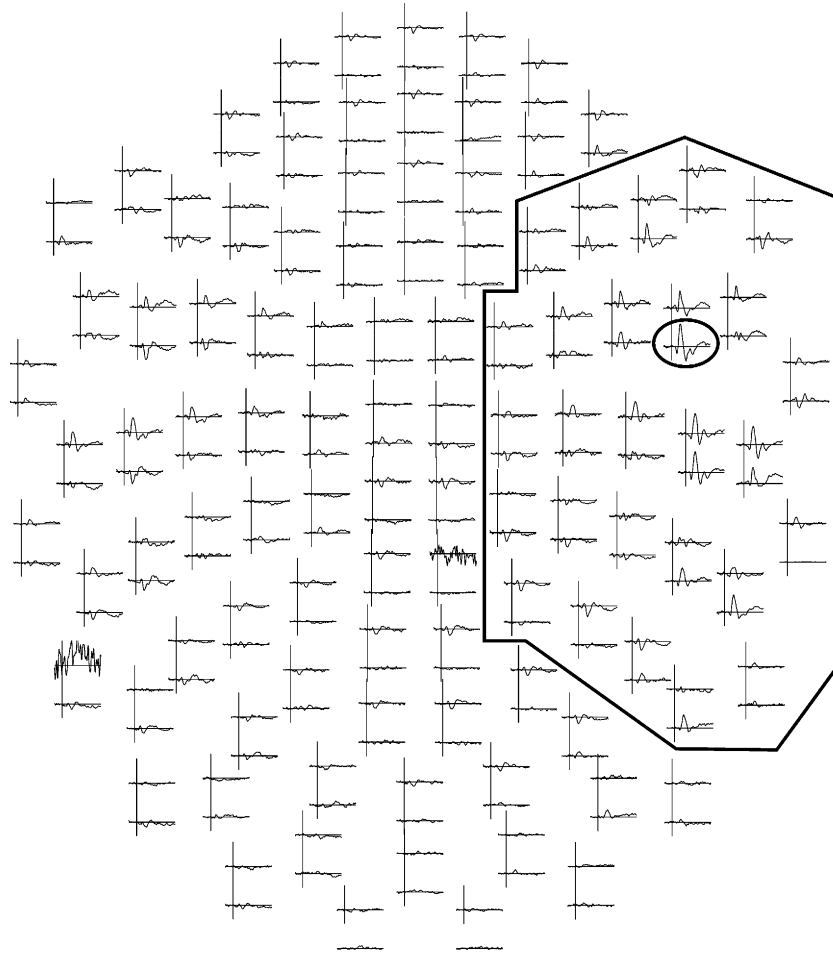
Fig. 2. The grand-averaged responses of the MEG gradiometer sensors. The auditory responses were more pronounced in the right hemisphere than in the left. The bordered area shows the 54 sensors used in response source-weighting (RSW) filter. The sensor depicted in Fig. 3 is encircled.

This is the central frequency of the simulated oscillations and also corresponds to the approximate frequency of the transient responses. The simulation time windows (−1.0 to 1.0 s) were sufficiently long to avoid edge artefacts within the examined time window (−100 to 300 ms). The wavelet power spectra from the MEG data (Fig. 4) were calculated using 1000-ms data windows (starting 500 ms before stimulus onset) after EOG rejection (see above). We used second-derivative-of-Gaussian ("Mexican hat") wavelets, which have a high temporal resolution. The center pass-band frequency of the wavelets was set at a spacing of 1 Hz. Edge artefacts were eliminated by discarding the first and last 100 ms of the wavelet-transformed data as well as the data of the lowest frequency (1 Hz). The single-trial wavelet power spectra were averaged over trials and subjects. The data of each frequency were divided the mean of the prestimulus (−400 to 0 ms) baseline power for that frequency and the data were further thresholded with a value of 1.3. The wavelet spectral power increases shown in the colored areas of Fig. 4. were at least seven times larger than the standard deviations of the baseline power of the corresponding frequencies (for normally distributed data, this corresponds to $P < 10^{-12}$).

For calculating the standard deviations of the amplitude, the unaveraged data were first band-pass filtered (according to bands depicted in Fig. 5) and then divided into 800-ms time windows. EOG artefact rejection was carried out by the procedure described

above. The accepted trials of each subject were collected into a matrix (each 800-ms trial forms a row of the matrix) from which the standard deviations were calculated for each time point. For statistical analyses, the standard deviation at the N1m latency was obtained separately from each subject by calculating the mean of the amplitude variance in a 50-ms time window centered at the peak latency of the grand-averaged N1m. These mean values were normalized using the mean of the baseline (−400–0 ms) and compared with the mean values from a 350- to 400-ms time window normalized in the same manner.

Results

Auditory stimuli elicited a characteristic series of deflections in the averaged signal, the most prominent being the N1m response peaking at around 100 ms after stimulus onset (Fig. 3a) and generated in the auditory cortex (Fig. 3b and c). In all subjects, the right hemisphere (Fig. 2) generated more prominent responses than the left ($F[1,8] = 13.5$, $P < 0.01$) and was used in further analyses. The RSW filter improved the S/N of the N1m against 50 Hz mains noise (frequency band 47–53 Hz) by 95%, compared to the average S/N obtained from the sensor pair with the highest N1m amplitudes in the averaged signal ($F[1,8] = 26.9$, $P < 0.001$). In the 1–45 Hz band, the improvement in the
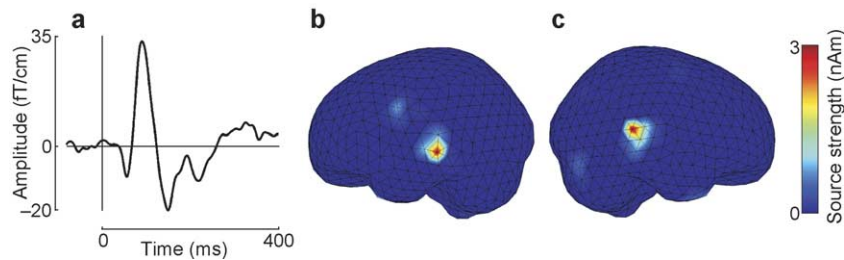
Fig. 3. Grand-averaged activity elicited by auditory stimulation. (a) A single-sensor response above the right temporal area showing a prominent N1m response peaking at around 100 ms. The sources of the N1m were focal both in the left (b) and right (c) hemispheres.

S/N rate was 15% ($F[1,8] = 12.2$, $P < 0.01$). The RSW filter was more effective against 50 Hz noise than against activity in the 1–45 Hz band ($F[1,8] = 19.7$, $P < 0.01$), which indicates that activity in the 1–45 Hz frequency band was mainly of cortical origin.

In all subjects, auditory stimulation increased the spectral power of the poststimulus unaveraged data compared to ongoing prestimulus brain activity (average increase 20%; $F[1,8] = 10.8$, $P \leq 0.01$). These increases were associated with transient auditory responses peaking at around 50, 100, and 200 ms (P1m, N1m, and P2m, respectively), and extending over frequencies 3–40 Hz at the latency of the N1m response (Fig. 4).

Phase synchronization of ongoing brain activity is one possible mechanism for the generation of event-related responses. That is, following the onset of a sensory stimulus the phase distribution of ongoing activity changes from uniform to one which is centered around a specific phase (Penny et al., 2002; see also Fig. 1a–d). Although the phase of a nonstationary broadband signal is poorly defined, the phase organization of MEG or EEG data can be examined by using trial-to-trial amplitude variance over time: phase synchronization can produce an above-baseline transient waveform in the averaged signal only if the amplitudes of the oscillatory processes do not have a uniform distribution, but rather, one that is reduced compared to that of the baseline during the transient waveform. Therefore, the trial-to-trial standard deviations of the signal amplitudes were calculated over the trial window in the 1–45 Hz frequency band and in the sub-bands 1–8 Hz, 8–15 Hz, 15–30 Hz, and 30–45 Hz. These frequency bands correspond approximately to the division into theta, alpha, beta, and gamma rhythms. In all the frequency bands, the standard deviations of the amplitudes remained stable throughout the trial duration (Fig. 5), although in the 1–45 Hz band an increase of 6% ($F[1,8] = 5.6$, $P < 0.05$) was observed at the latency of the N1m response. Thus, ongoing brain activity is not in a coherent phase when the auditory ERR occurs, and phase synchronization can be ruled out as an explanation of ERR generation.

The relationship between ongoing brain activity and the N1m response was further investigated by sorting single-trial MEG responses into low, medium, and high spectral power
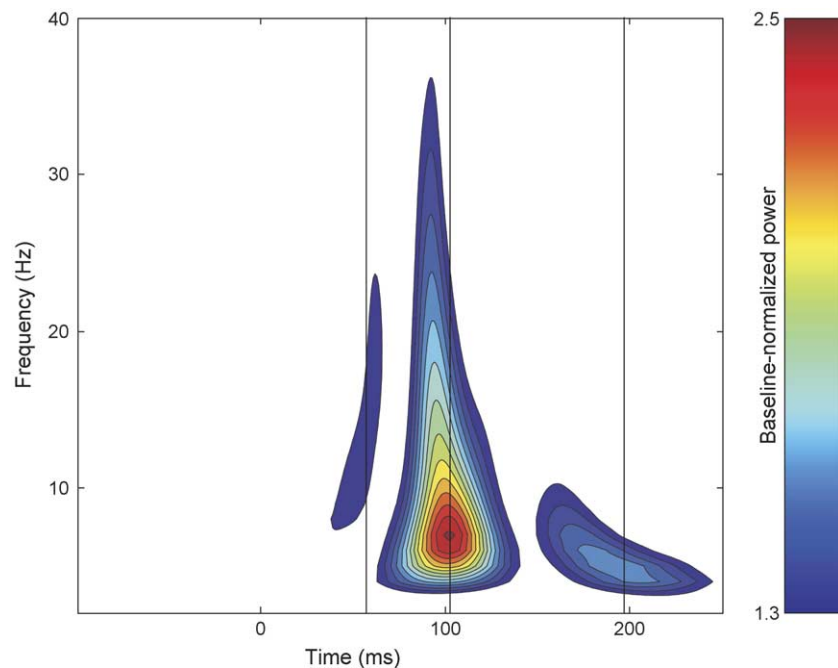
Fig. 4. Wavelet spectral power characterization of auditory event-related responses. The power on each frequency, obtained from unaveraged RSW-filtered data, was divided with the mean of the baseline power from the same frequency in order to obtain a frequency-specific signal-to-noise ratio. Using thresholding at 30% increase in signal power, only the three auditory responses P1m, N1m, and P2m are observable (vertical lines indicate their respective peak latencies).
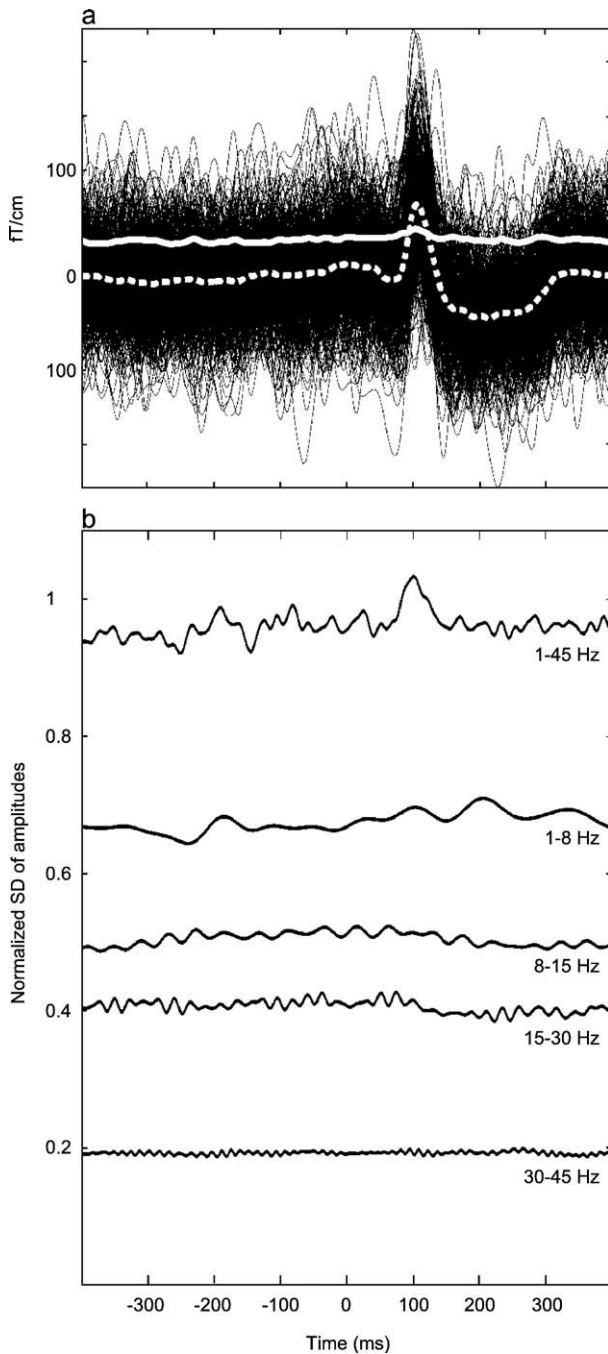
Fig. 5. The standard deviation of amplitudes over trials as a function of time. In (a), data from all the trials from a single subject at 1–45 Hz band are shown (black curves). The dotted white curve is the averaged response. The solid white curve is the standard deviation of the amplitudes of the trials. The standard deviation does not show a decrease at the time of the event-related responses which would indicate phase synchronization. The distribution of the curves resembles that of the additive component model in Fig. 1f rather than that of the phase reorganization model in Fig. 1a. In (b), the grand-averaged standard deviation profiles (normalized according to the N1m peak amplitude) indicate that no phase synchronization and subsequent reduction in the standard deviation occurs in any of the frequency bands (see Fig. 1). Instead, there is a slight increase in standard deviation at the 1–45 Hz band at the latency of the N1m (approximately 100 ms). This increase can be accounted for by the trial-to-trial variance of the N1m response which is additional to the variance of the ongoing brain activity.

groups of equal size. The data were averaged separately for each group and the peak amplitudes and latencies of the N1m responses were determined. This procedure was carried out separately for the pre- and poststimulus time windows in the five frequency bands defined above. No effect of baseline spectral power was found in the amplitude or latency of the N1m response in any of the frequency bands (all $P = $ ns), while in all frequency bands the spectral power differences were highly significant between the three spectral-power groups ($F[2,16] \geq 15$, $P < 0.001$). In examining poststimulus spectral power, we found that trials with high spectral power coincided with trials with large N1m amplitude in the 1–45 Hz ($F[2,16] = 44.8$, $P < 0.001$), 1–8 Hz ($F[2,16] = 47.0$, $P < 0.001$), 8–15 Hz ($F[2,16] = 40.0$, $P < 0.001$) and 15–30 Hz ($F[2,16] = 6.5$, $P < 0.01$) frequency bands. This can be explained through stochastic superposition of ongoing activity and N1m, which results in trials of high- and low-spectral power (black and gray curves in Fig. 1e and j, respectively), with the ongoing oscillation being in either a dampening or enforcing phase in relation to the N1m. When the wavelength of the ongoing oscillation is much shorter than the width of the N1m response (approximately 60 ms), this effect becomes unobservable and, consequently, in the 30–45 Hz frequency band we found that poststimulus spectral power had no effect on the amplitude of the N1m ($P = $ ns).

Discussion

The relationship between ongoing brain activity and human auditory event-related responses (ERRs) was explored with MEG. The spectral power of unaveraged poststimulus activity was 20% larger than that of prestimulus activity and this increase could be attributed to the elicitation of ERRs. Importantly, we found that the phase of ongoing activity was in no coherent phase at any time before or after stimulus presentation. In the light of these observations, phase synchronization is an inadequate explanation of ERR generation, which would appear to be independent of ongoing brain activity.

By sorting single trials according to poststimulus spectral power, we observed a strong effect of spectral power on the amplitude of the N1m response. Such a dependence has previously been taken to indicate that ERRs and ongoing activity are interlinked (Makeig et al., 2002). Yet, as shown in Fig. 1e and j, this effect can also be caused by stochastic superposition of ongoing activity and independent ERRs. If the two were due to interrelated processes, prestimulus spectral power should have an effect on the ERRs. However, we found no such effect on the N1m amplitude or latency. Thus, our results indicate a high degree of independence between ongoing brain activity and auditory ERRs. In conditions where the subject's vigilance varies or in cognitive tasks which are reflected in oscillatory brain responses, however, the mutual sensitivity of ongoing brain activity and ERRs to the arousal and/or cognitive state may lead to correlations between the types of brain activity without proving causality between the two.

For phase synchronization of ongoing brain activity to underlie the emergence of the N1m response, a decrease in the trial-to-trial amplitude variance of brain activity should be observed at the N1m latency. Instead of this, we found a slight variance increase (Fig. 5), which can be accounted for by the

trial-to-trial amplitude variance of the N1m which is additional to that of ongoing activity. This increase was observable only in the 1–45 Hz frequency band which is explained by the N1m responses being either due to a unitary process or composed of several processes which are temporally aligned and span a wide frequency range (Fig. 4). In both cases, when the N1m is decomposed into several frequency bands, the variances of the amplitudes gained in the different frequency bands sum linearly to produce the variance of the amplitude of the original signal. In contrast, the phases of the ongoing oscillations in different frequency bands are non-aligned, as shown by the amplitude variance of the ongoing activity in 1–45 Hz band being less than the sum of the sub-band amplitude variances (Fig. 5). Therefore, the variance of the N1m sums linearly over the frequency bands whereas that of ongoing activity fails to do so, leading to the observed result.

Previous suggestions that ERRs are produced by phase synchronization of ongoing activity were based on EEG data (Başar, 1980; Jansen et al., 2003; Makeig et al., 2002; Sayers et al., 1974). The discrepancy between these suggestions and our results is unlikely to be due to differences between EEG and MEG. Both reflect the activity of the same primary current generators (Hämäläinen et al., 1993), and recent evidence indicates that MEG appears to be sensitive to all but deepest of mass-activity brain sources (Hillebrand and Barnes, 2002). Previous studies have drawn on either negative results (Sayers et al., 1974), possibly caused by a low signal-to-noise ratio (avoided here by the experimental design and the use of RSW), or have employed phase analysis methods (Jansen et al., 2003; Makeig et al., 2002) which fail to discriminate between phase synchronization and signal modulation due to transient additive responses (see Fig. 1). Also, it has been pointed out that a correlational link between ongoing activity and ERRs (Başar, 1980) does not in itself imply causality (Jansen et al., 2003). Further, while the brain dynamics of different sensory modalities may differ from each other, results gained in the somatosensory system (Bijma et al., 2003) showing that ongoing activity was unaffected by median nerve stimulation support our conclusions.

The idea that stimulus-evoked responses are additional to ongoing activity gains support from intracortical animal studies. Firstly, cortical cells respond to auditory stimulation by increasing or decreasing their firing rates (e.g., Brosch and Schreiner, 1997, 2000). Secondly, multi-unit studies indicate that ERR generation is due to a complex series of cross-laminar sink-source configurations triggered by the stimuli and accompanied by increases in multi-unit activity (Arezzo et al., 1986; Vaughan et al., 1986). Thirdly, intracranial (Arieli et al., 1996) and intracellular (Azouz and Gray, 1999) measurements suggest that the trial-to-trial variability of evoked responses can be explained through linear superposition of ongoing activity and the evoked response, with the ongoing dynamics being unaffected by the evoked response. Finally, the suggestion that phase synchronization underlies ERRs is problematic from a neural information processing perspective because ongoing oscillations would stochastically, and thus without sensory stimuli, produce a state analogous to the stimulus-induced synchronized state. This problem does not arise with stimulus-evoked responses being additional to ongoing activity. In resolving the fundamental problem of the relationship between ongoing and evoked brain activity, our observations and methodology may turn out to be useful to the future develop-ment of electrophysiological measures both in basic research and for practical purposes.

References

Addison, P.S., 2002. The Illustrated Wavelet Transform Handbook. IOP Press, Bristol and Philadelphia.

Arezzo, J.C., Vaughan Jr., H.G., Kraut, M.A., Steinschneider, M., Legatt, A.D., 1986. Intracranial generators of event related potentials in the monkey. In: Cracco, R.Q., Bodis-Wollner, I. (Eds.), Evoked potentials frontiers of clinical neuroscience vol. 3. Alan R. Liss, New York, pp. 174–189.

Arieli, A., Sterkin, A., Grinvald, A., Aertsen, A., 1996. Dynamics of ongoing activity: explanation of the large variability in evoked cortical responses. Science 273, 1868–1871.

Azouz, R., Gray, C.M., 1999. Cellular mechanisms contributing to response variability of cortical neurons in vivo. J. Neurosci. 19, 2209–2223.

Başar, E., 1980. EEG-Brain Dynamics: Relation Between EEG and Brain Evoked Potentials. Elsevier, New York.

Bijma, F., de Munck, J.C., Huizenga, H.M., Heethaar, R.B., 2003. A mathematical approach to the temporal stationarity of background noise in MEG/EEG measurements. NeuroImage 20, 233–243.

Brandt, M.E., Jansen, B.H., Carbonari, J.P., 1991. Pre-stimulus spectral EEG patterns and the visual evoked response. Electroencephalogr. Clin. Neurophysiol. 80, 16–20.

Brosch, M., Schreiner, C.E., 1997. Time course of forward masking tuning curves in cat primary auditory cortex. J. Neurophysiol. 77, 923–943.

Brosch, M., Schreiner, C.E., 2000. Sequence sensitivity of neurons in cat primary auditory cortex. Cereb. Cortex 10, 1155–1167.

Coenen, A.M.L., 1998. Neuronal phenomena associated with vigilance and consciousness: from cellular mechanisms to electroencephalographic patterns. Conscious. Cogn. 7, 42–53.

Hämäläinen, M., Hari, R., Ilmoniemi, R.J., Knuutila, J., Lounasmaa, O.V., 1993. Magnetoencephalography—Theory, instrumentation, and applications to noninvasive studies of the working human brain. Rev. Mod. Phys. 65, 413–497.

Hillebrand, A., Barnes, G.R., 2002. A quantitative assessment of the sensitivity of whole-head MEG to activity in the adult human cortex. NeuroImage 16, 638–650.

Jansen, B.H., Agarwal, G., Hegde, A., Boutros, N.N., 2003. Phase synchronization of the ongoing EEG and auditory EP generation. Clin. Neurophysiol. 114, 79–85.

Laufs, H., Krakow, K., Sterzer, P., Eger, E., Beyerle, A., Salek-Haddadi, A., Kleinschmidt, A., 2003. Electroencephalographic signatures of attentional and cognitive default modes in spontaneous brain activity fluctuations at rest. Proc. Natl. Acad. Sci. U. S. A. 100, 11053–11058.

Makeig, S., Westerfield, M., Jung, T.P., Enghoff, S., Townsend, J., Courchesne, E., Sejnowski, T.J., 2002. Dynamic brain sources of visual evoked responses. Science 295, 690–694.

Mäkinen, V.T., May, P.J.C., Tiitinen, H., 2004. Human auditory event-related processes in the time-frequency plane. NeuroReport 15, 1767–1771.

Mallat, S.A., 1998. Wavelet Tour of Signal Processing. Acad. Press, San Diego.

Näätänen, R., Picton, T.W., 1987. The N1 wave of the human electric and magnetic response to sound: a review and an analysis of the component structure. Psychophysiology 24, 375–425.

Penny, W.D., Kiebel, S.J., Kilner, J.M., Rugg, M.D., 2002. Event-related brain dynamics. Trends Neurosci. 25, 387–389.

Percival, D.B., Walden, A.T., 1993. Spectral Analysis for Physical Applications: Multitaper and Conventional Univariate Techniques. Cambridge Univ. Press, Cambridge.

Rahn, E., Başar, E., 1993a. Prestimulus EEG-activity strongly influences the auditory evoked vertex response: a new method for selective averaging. Int. J. Neurosci. 69, 207–220.

Rahn, E., Başar, E., 1993b. Enhancement of visual evoked potentials by stimulation during low prestimulus EEG stages. Int. J. Neurosci. 72, 123–136.

Sayers, B.M., Beagley, H.A., Henshall, W.R., 1974. The mechanism of auditory evoked EEG responses. Nature 247, 481–483.

Tesche, C.D., Uusitalo, M.A., Ilmoniemi, R.J., Huotilainen, M., Kajola, M., Salonen, O., 1995. Signal-space projections of MEG data characterize both distributed and well-localized neuronal sources. Electroencephalogr. Clin. Neurophysiol. 95, 189–200.

Tiitinen, H., Sinkkonen, J., Reinikainen, K., Alho, K., Lavikainen, J., Näätänen, R., 1993. Selective attention enhances the auditory 40-Hz transient response in humans. Nature 364, 59–60.

Torrence, C., Compo, G.P., 1998. A practical guide to wavelet analysis. B. Am. Meteorol. Soc. 79, 61–78.

Uutela, K., Hämäläinen, M., Somersalo, E., 1999. Visualization of magnetoencephalographic data using minimum current estimates. NeuroImage 10, 173–180.

Varela, F.J., Lachaux, J.-P., Rodriguez, E., Martinerie, J., 2001. The brainweb: phase synchronization and large-scale integration. Nat. Rev. Neurosci. 2, 229–239.

Vaughan Jr., H.G., Weinberg, H., Lehmann, D., Okada, Y., 1986. Approaches to defining the intracranial generators of event-related electrical and magnetic fields. Electroencephalogr. Clin. Neurophysiol. Suppl. 38, 505–544.

Vrba, J., Robinson, S.E., 2001. Signal processing in magnetoencephalography. Methods 25, 249–271.